551.511.32 : 551.513.1

A problem in baroclinic stability

By J. S. A. GREEN
Imperial College, London

(Manuscript received 26 February 1959; in revised form 18 December 1959)

SUMMARY

Linearized equations are used to formulate the theoretical problem of the stability of large-scale zonal flow with vertical shear. The problem is solved in some generality and illustrates the connexion between the solutions already obtained by Rossby, Charney and Eady.

1. INTRODUCTION

The purpose of this study is to extend the class of stability problems as posed by Charney (1947) and Eady (1949). A broad steady zonal baroclinic current is perturbed by a small-amplitude large-scale wave motion. Consideration of the stability characteristics of this system yields information concerning the initial stages in the growth of baroclinic disturbances.

The equations are simplified so that only those processes directly relevant to the scale of motion are included. The appropriate analysis has already been given in detail (see, e.g., Eady 1949) and will not be repeated here, although the principal steps are indicated.

The main assumptions are that the fluid is frictionless, the motion adiabatic, and that the Richardson number $Ri = gB \Big/ \left(\frac{dU}{dZ}\right)^2$ is large and positive. It can then be shown that the horizontal motion is nearly geostrophic, and that the appropriate vorticity equation (Eady 1949, p. 47, Eqs. 8 and 16) is of the form

$$\frac{D\zeta}{Dt_h} + v\beta = \frac{f}{\rho}\frac{\partial}{\partial Z}(\rho w) \quad . \quad . \quad . \quad . \quad (1)$$

where the suffix h denotes horizontal and

$\frac{D}{Dt_h}$ = differentiation following the horizontal motion

ζ = vertical component of relative vorticity

v = meridional velocity

$\beta = \frac{\partial f}{\partial y}$ = latitude variation of the Coriolis parameter

ρ = density

Z = height

w = vertical velocity

It is convenient to assume a ' standard ' distribution of density with height $\rho_0(Z)$ and the corresponding static pressure $P_0(Z)$, such that they describe the mean state of the fluid. We then consider the pressure and density fields as being given by the standard value plus a deviation, and note that the deviations consistent with the observed large-scale tropospheric motion are much smaller than the mean values.

Thus we write, pressure $= P_0(Z) + \delta P(x, y, Z, t)$

density $= \rho_0(Z) + \delta\rho$

and entropy$/C_p = C_v/C_p \log P - \log \rho \simeq \phi_0(Z) + \delta\phi$

with $\delta\phi/\phi_0 \ll 1$

The conservation of entropy can then be written

$$\frac{D}{Dt_h}\delta\phi + Bw = 0 \quad . \quad . \quad . \quad . \quad . \quad (2)$$

where

$$B = \frac{d\phi_0}{dZ}$$

It is supposed that the deviation pressure and density fields are in static equilibrium

$$\frac{\partial}{\partial Z}\delta P + g\,\delta\rho = 0 \quad . \quad . \quad . \quad . \quad . \quad (3)$$

This set of equations, together with the geostrophic approximation, allows us to eliminate all the dependent variables in terms of the deviation pressure and defines the model fluid. It is, however, more convenient to write the equations in terms of the dimensionsionless function ψ defined by

$$\delta P = \rho_0(Z)\, gH\, \psi(x, y, Z, t)$$

where H is a geometric scale height. The geostrophic approximation becomes

$$\mathbf{V}_h = \frac{gH}{f}\mathbf{k} \wedge \nabla\psi$$

(where $\mathbf{k}$ is unit vertical vector)

and

$$\delta\phi = H\frac{\partial\psi}{\partial Z} - HB\,\psi \simeq H\frac{\partial\psi}{\partial Z}$$

Note that ψ behaves like the classical 'non-divergent' stream function in the horizontal, but with the vertical gradient corresponding (very nearly) to log potential temperature.

Eq. (1) becomes

$$\frac{D}{Dt_h}\left\{\frac{\partial^2\psi}{\partial x^2} + \frac{\partial^2\psi}{\partial y^2} + \frac{f\beta}{gH}y + \frac{f^2}{gB}\left(\frac{\partial^2\psi}{\partial Z^2} + \frac{1}{\rho_0}\frac{\partial\rho_0}{\partial Z}\frac{\partial\psi}{\partial Z}\right)\right\} = 0 \quad . \quad . \quad (4)$$

and

$$w = -\frac{H}{B}\frac{D}{Dt_h}\frac{\partial\psi}{\partial Z} \quad . \quad . \quad . \quad . \quad . \quad (5)$$

We now consider a steady zonal baroclinic motion $U(Z)$ disturbed by a small-amplitude perturbation. It is convenient to specify the perturbation in the form :

$$\text{perturbation } \psi = \text{Real part of } \left\{F(Z)\exp i\lambda(x - Ct)\begin{matrix}\sin\\ \cos\end{matrix}\mu y\right\}$$

Where $F(Z)$ is a complex function describing both the phase and amplitude of ψ, and the complex number $C = C_r + iC_i$ describes the phase velocity C_r and rate of amplification $\exp \lambda C_i t$ of the perturbation. The coordinate system is rectangular with the x-axis horizontal and directed towards the East, the y-axis horizontal and directed towards the North and the z-axis vertical. The variation of the map-scale with latitude has been

neglected as is customary in meteorological dynamics. Thus λ is the east-west wave number, and μ is the South-North wave number. It is convenient to re-write the equation in non-dimensional form and we therefore define

$$z = Z/H \text{ where } H \text{ is a geometric scale height in the fluid}$$

$$u = U(Z)/\Delta U \text{ where } \Delta U \text{ is a typical velocity difference}$$

$$c = C/\Delta U \text{ wave velocity}$$

$$p^2 = \frac{gB}{f^2} H^2 (\lambda^2 + \mu^2) \text{ horizontal wave-number}$$

$$\kappa = -\frac{H}{\rho_0}\frac{d\rho_0}{dZ} \text{ mass divergence parameter}$$

$$\gamma = \frac{gB}{f^2} H^2 \frac{\beta}{\Delta U} \text{ generalized } \beta \text{ parameter}$$

The non-dimensional perturbation form of Eq. (4) then becomes :

$$(u - c)(F'' - \kappa F' - p^2 F) + (\gamma + \kappa u' - u'') F = 0 \quad . \quad . \quad (6)$$

where the primes denote differentiation with respect to z, and the function F defines the perturbation quantities via

$$\text{perturbation pressure} = \rho_0(Z)\, gH \text{ Real part } \left\{F(z) \exp i\lambda (x - Ct) \begin{matrix}\sin \\ \cos\end{matrix} \mu y\right\}$$

2. The parameters of the motion

For the ranges of pressure and temperature in which we are interested, the fluid must be considered as compressible and this affects three distinct physical processes :

(*i*) The ' dynamic compressibility ' is associated with the elastic forces in the equations of motion and sound waves. The speed of sound is much greater than the wave speeds with which we are concerned and this type of compressibility has been excluded (effectively by making the speed of sound in the model infinite).

(*ii*) The ' static stability ' is a measure of the static forces that oppose vertical movement and is represented by the vertical gradient of entropy (or of potential density), not by the gradient of temperature (or density) only.

(*iii*) The ' mass divergence ' effect is associated with the variation in the volume of a given mass of fluid. The vorticity equation contains a term $f \operatorname{div} \mathbf{V}_h$ that cannot be determined accurately by using the geostrophic approximation. Hence the continuity equation is used, in the form :

$$\operatorname{div} \mathbf{V}_h + \frac{\partial w}{\partial Z} = -\frac{1}{\rho}\frac{D\rho}{Dt} \simeq -\frac{w}{\rho_0}\frac{d\rho_0}{dZ}$$

Thus the difference between the continuity (or divergence) of mass and volume is expressed in terms of $\kappa = -\frac{H}{\rho_0}\frac{d\rho_0}{dZ}$, which is referred to as the mass divergence parameter.

The horizontal scale of the motion is represented by the non-dimensional parameter p, and $\lambda^2 + \mu^2$ appears in that combination throughout, except for the amplification which is represented by a factor $\exp \lambda C_i t$. It follows that if all the parameters of the motion except μ are fixed, then the rate of amplification will be a maximum when $\mu = 0$. This is assumed throughout so that the perturbation motion consists of troughs and ridges of infinite North-South extent. This is not a particularly apt approximation because of the distortion of the coordinate system in extreme latitudes. It might be added that baroclinic zones are observed to be of small meridional extent. However, other studies (e.g., Eady 1949) have indicated the kind of modification to be expected in these more realistic cases.

In defence of the present theory it might be noted that $\mu = 0$ in this context really implies $\mu \ll \lambda$ and that the perturbation for any μ can be recovered from the solutions given here. The most significant advantage is that with $\mu = 0$ the perturbation solution is (technically) a solution of the full non-linear Eq. (4). Thus the transport properties calculated from correlations between the linearized (first order) quantities are not distorted by contributions from second-order effects.

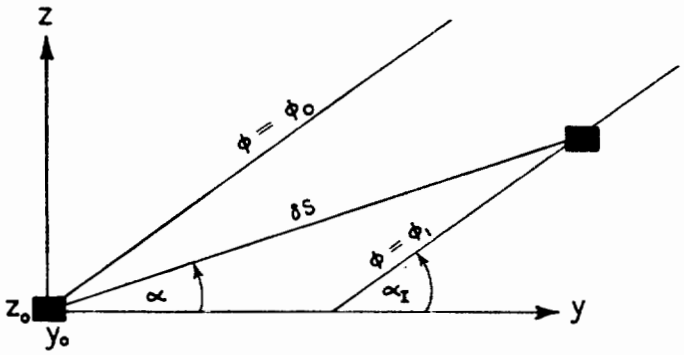

Figure 1. Schematic meridional section of the field of motion, showing the unperturbed adiabatics, and illustrating the parcel interchange.

In the unperturbed system there is potential energy which is available for conversion into perturbation kinetic energy. Let the (unperturbed) entropy gradients at some point (y_0, Z_0) be $\frac{\partial \phi}{\partial y} = -A$, $\frac{\partial \phi}{\partial Z} = B$ with the isentropic slope $\alpha_I = A/B$ (see Fig. 1). Now suppose that we take a mass M_0 of fluid from (y_0, Z_0) to $(y_0 + \delta S \cos \alpha, Z_0 + \delta S \sin \alpha)$ and return the displaced mass M_1 to (y_0, Z_0). Then neglecting the change in the mean pressure field, the change in the potential energy is

$$\Delta = g\, \delta S \sin \alpha\, (M_0 - M_1)$$

If this interchange is carried out adiabatically so that the parcel of mass M_0 is associated with entropy ϕ_0 throughout then

$$M_1/M_0 = \exp(\phi_0 - \phi_1)$$

and

$$\Delta = gM\, (\delta S)^2 \sin \alpha\, (B \sin \alpha - A \cos \alpha) + 0\,(\delta S)^3 \quad . \quad . \quad (7)$$

where

$$2M = M_0 + M_1$$

We see that for a given δS the maximum energy release occurs when $\alpha \simeq \frac{1}{2} \alpha_I$ and is given by

$$\Delta_{\max} = -gM\, (\delta S)^2 \frac{A^2}{4B} = -\frac{M\,(\delta S)^2}{4} \frac{f^2}{gB} \left(\frac{\partial U}{\partial Z}\right)^2 \quad . \quad . \quad (8)$$

assuming $\alpha_I \ll 1$, and $A \delta S \ll 1$.

We suppose this interchange to be consistent with an exponentially amplifying motion whose horizontal speed is given by, say : $V = \delta V \exp \lambda C_i\, t$ and displacement $\delta S = \int_{-\infty}^{t} V\, dt$

The change in the kinetic energy of this motion is given by :

$$\Delta_{\text{obs}} = 2\,(\tfrac{1}{2} M\, (\lambda C_i\, \delta S)^2) = (2p\, c_i)^2\, \Delta_{\max}$$

We see that pc_i is a measure of the efficiency of conversion of potential into kinetic energy, a more refined analysis confirming the maximum possible value of 0·5.

The variation of the Coriolis parameter with latitude appears in the ' generalized β parameter ' γ, together with the unperturbed entropy gradients. With α_I as the slope of the unperturbed isentropics, we can write

$$\gamma = \frac{H\beta}{f\alpha_I} = v\beta \Big/ \frac{v\alpha_I}{H} f$$

Now the paths of particles in the meridional plane tend to have the ' optimum ' slope of $\frac{1}{2}\alpha_I$ in the middle levels of the fluid. Hence $v\alpha_I/H$ is an estimate of $\frac{\partial w}{\partial Z}$, and $v\alpha_I f/H$ is the corresponding rate-of-change of vorticity due to the vortex stretching. Thus the generalized β parameter gives a measure of the effect of the variation of the Coriolis parameter with latitude, in comparison with that of the baroclinic vortex stretching, in producing vorticity changes.

The solutions to Eq. (6) cannot in general be expressed in analytic form. Even in the special case $u = z$, when such a solution is possible (see Charney 1947; Kuo 1952) the labour involved in calculating the eigen values by hand is prohibitive. Accordingly, it was decided that a high-speed computing device was necessary, and this being so, the solution should remain in numerical form throughout. The actual technique employed is not relevant here although a short account is given in § 7.

3. Linear velocity profile

If the entropy gradients are independent of height (A and B constant), and if we neglect the mass divergence effect (put $\kappa = 0$), then Eq. (8) shows that potential energy would be equally available everywhere were it not for constraints of a kinematic nature. An assessment of the simplest possible constraints that can limit the motion has led to two previous analyses of this problem. We are not concerned at this point with the details of these treatments, so that only their essential features are indicated.

Charney (1947) and Kuo (1952) considered the fluid to be bounded below by a rigid horizontal surface but unlimited above. They found that if the shear is westerly and β positive, then growing waves are possible.

Eady (1949) considered the fluid to be bounded, above and below by rigid horizontal surfaces and found growing waves with $\beta = 0$.

These simplifications illustrate the decisive nature of the constraints, for if we remove the upper lid in Eady's treatment or put $\beta = 0$ in Charney's, the problems become identical, and all waves are neutral. Thus the motion is rendered unstable by the action of these constraints.

4. Linear profile – β effect

The work of this section describes the transition from the Eady to the Charney solution, for motion between two rigid boundaries as the β-effect becomes important. We suppose the motion to be bounded, above and below by smooth, rigid, horizontal surfaces, and neglect the mass divergence effect (put $\kappa = 0$).

If $\gamma = 0$ (Eady), then for each wavelength there are two solutions. For long wavelengths this pair of solutions corresponds to amplifying and diminishing waves travelling with the mean velocity of the undisturbed flow. All the wave properties are either symmetrical or anti-symmetrical about the mid-level of the fluid, and the growth-rate is a maximum at a finite wavelength. Very short waves are neutral, and the pair of solutions then correspond to waves whose steering levels are displaced symmetrically about the mid-level (see Figs. 2 and 5).

With $\gamma \neq 0$, the differential equation is no longer symmetrical, and calculation shows that :

(*i*) There exists a growing wave for nearly all wavelengths – there is no short-wave limit to instability;

(*ii*) An additional long-wave solution is possible;

(*iii*) If $\gamma > 0$ ($\beta > 0$ and westerly shear), then the steering level is below the mid-level for all wavelengths.

In describing the nature of these results it is convenient to *make* a distinction between what may be loosely called thermodynamic, and kinematic processes. If the motion is to make a release of potential energy possible then particle paths must have (on the average) a slope between that of the isentropics and the horizontal. This is a necessary condition because all other orientations of particle paths would require work to be done against the static stability (see, for example, Eq. 7). It is not a sufficient condition because the relative phase of the temperature and velocity fields is not specified.

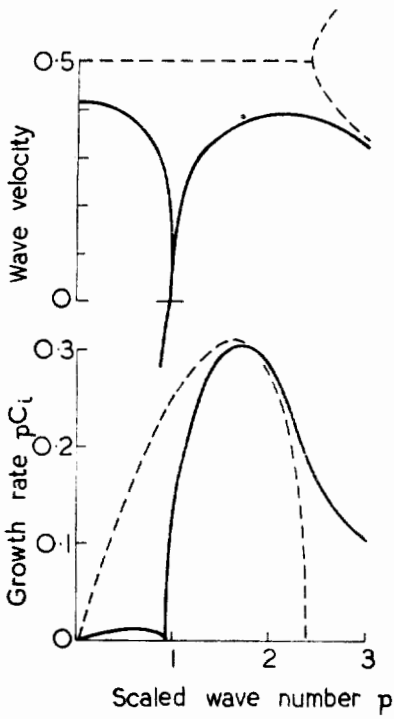

Figure 2. Growth-rate pc_i, and wave velocity c_r as a function of wave number for the linear profile $u = z$.
$\gamma = 0$ (dashed line) $\gamma = 0{\cdot}5$ (full line)
The wave-speed is equal to the height of the steering level/fluid depth.

The appropriate vorticity equation ($\kappa = 0$) expresses a balance between the vorticity changes due to the horizontal advection of absolute vorticity and those derived from the stretching of the vortex :

$$\frac{D\zeta}{Dt_h} + v\beta = f\frac{\partial w}{\partial Z}$$

Now for wavelike motion the first term in this equation is small relative to v near the steering level where (by definition) there is no zonal advection relative to the wave. Here then the

balances must be maintained between the vorticity changes due to meridional advection, and those due to the vortex stretching :

$$\text{i.e., } v\beta \simeq f\frac{\partial w}{\partial Z} \text{ at the steering level} \quad . \quad . \quad . \quad (9)$$

Now suppose that this steering level is near a lower lid. Then $w = 0$ at the lid, and $\frac{\partial w}{\partial Z} > 0$ for $v > 0$ at the steering level. Thus if $\frac{\partial w}{\partial Z}$ changes slowly in between, then $w > 0$ for $v > 0$ at the steering level, and a low steering level therefore implies $\overline{vw} > 0$. This is consistent with the necessary condition if the thermal wind is westerly. Whether this motion will be amplifying or diminishing depends on the phase difference between the velocity and temperature fields.

Conversely, steering level near an upper lid would imply $\overline{vw} < 0$ which does not satisfy the necessary condition with a westerly thermal wind, but does so if the thermal wind is easterly. Alternatively we can suppose that the correlation between v and w, *and* the variation of w with height are implied by the nature of the energy transformations and that the steering level satisfying the condition (9) is then selected.

This bias has an important effect on the short waves, for if $\gamma = 0$ the very short waves form a neutral pair with steering levels close to the boundaries. With $\gamma > 0$, the lower wave becomes an amplifying-diminishing pair, and there is no upper wave (see Fig. 2). If $\gamma < 0$ there is conversely no lower wave – a somewhat disconcerting state of affairs that may be of significance in numerical forecasts since the large-phase velocity of an upper wave could lead to computational instability.

A third major effect arising when $\beta \neq 0$ is the existence of a critical wavelength for which the waves are neutral, and stationary relative to the surface wind. For shorter wavelengths there is a pair of solutions corresponding to growing and diminishing waves, but for longer (than critical) wavelengths there are at least three solutions. Two form a conjugate pair as before, but with rather different structure and a much smaller growth-rate. The third solution is neutral and moves retrograde with respect to the surface wind.

If the fluid is deep or the shear small (i.e., γ large), then other critical points may occur at longer wavelengths, and at each critical point an additional neutral wave is encountered. For example, in the problem discussed by Charney, the fluid depth was infinite, and there are an infinite number of critical wavelengths – corresponding to polynomial solutions of his differential equation.

This behaviour of the longer waves is best appreciated by considering the form of the perturbation equation :

$$(z - c)(F'' - p^2 F) + \gamma F = 0 \quad . \quad . \quad . \quad (10)$$

where the primes denote differentiation with respect to the scaled height z. If the wavelength is large then $p^2 \ll 1$, so that in order to balance the last term, $F'' - p^2 F$ can be small if $(z - c)$ is large, that is, c must be large, and the variation of $(z - c)$ is then irrelevant. Thus we identify an inertial wave with a phase velocity $c \simeq -\gamma/p^2$ i.e. a Rossby wave.

An alternative is that F''/F should be large compared to p^2, and c finite, or that the motion should balance the vorticity changes due to meridional advection and vortex stretching at *all* heights, or

$$v\beta \simeq f\frac{\partial w}{\partial Z} \text{ for all } Z.$$

This is a very stringent constraint for :

$$vw \simeq \frac{f}{\beta}\frac{\partial}{\partial Z}(\tfrac{1}{2}w^2)$$

Thus the total $\int_0^H vw\,dz$ between rigid lids is zero. In fact the correlation between v and

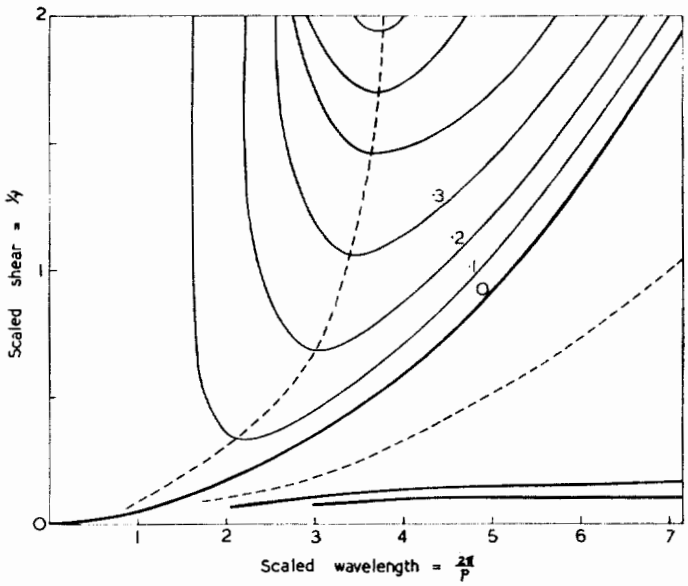

Figure 3. The variation of growth-rate as a function of wavelength and generalized β-parameter. Isopleths of pc_i/γ (growth-rate) against $1/\gamma$ (shear) and $2\pi/p$ (wavelength). All waves are unstable, or neutral (thick lines). The almost neutral waves ($1/\gamma < 0{\cdot}1$) have been omitted.

w is attained by a reversal of the meridional velocity in the upper layers. The necessary condition $\overline{vw} > 0$ is only just attained and the growth-rate is correspondingly small (Fig. 2 and 6).

The broad features of the growth-rate spectrum are illustrated in Fig. 3. The efficiency of conversion of potential energy into kinetic energy that is measured by pc_i maximized with respect to the wave-number p, is very insensitive to variations in the β-effect. For example, maximum pc_i is 0·310 at $\gamma = 0$, 0·286 at $\gamma = 10$. For comparison, maximum pc_i would be reduced to about 0·27 by a ' frictional boundary layer ' at the lower surface (kinematic eddy viscosity $= 10^5$ cm^2 sec^{-1}, $\Delta U = 30$ m sec^{-1}, $H = 10$ km, $(gB)^{\frac{1}{2}} = 10^{-2}$ sec^{-1}, $f = 10^{-4}$ sec^{-1} and $\gamma = 0$). The wavelength at which the maximum rate of growth occurs (the dominant wavelength) varies markedly with the shear, in the sense that longer waves are dominant when the shear is large. This is consistent with the general stabilisation of the longer waves arising when $\beta \neq 0$.

5. Linear profile – stratosphere

The solutions of Eq. (10) with a wavelength less than the first critical wavelength, have an exponential-type variation in the vertical, so that waves of large horizontal extent also extend, in general, to greater heights. Thus the upper boundary of a rigid lid is not ' realistic ' for the long waves and some calculations were therefore made with a superimposed semi-infinite layer of large static stability instead of the upper layer with infinite static stability (lid).

The unperturbed tropopause was supposed horizontal, the static stability of the stratosphere four times that of the troposphere, and the linear velocity profile was extended indefinitely upwards. It can be seen from Eq. (6) that with u increasing indefinitely with height, all solutions are ultimately of exponential form, so that only the decreasing solution is physically relevant. Further, even if u were to attain a finite value the solutions would be oscillatory only with c real, i.e., for critical waves only.

A decrease in the static stability of the upper layer results in an upward displacement of the steering level. With $B_S/B_T = 4$, and $\gamma = 0$ the speed of the dominant wave is 0·72 and maximum $pc_i = 0{\cdot}29$ in the units of Fig. 4. However, with $B_S/B_T = 4$ and

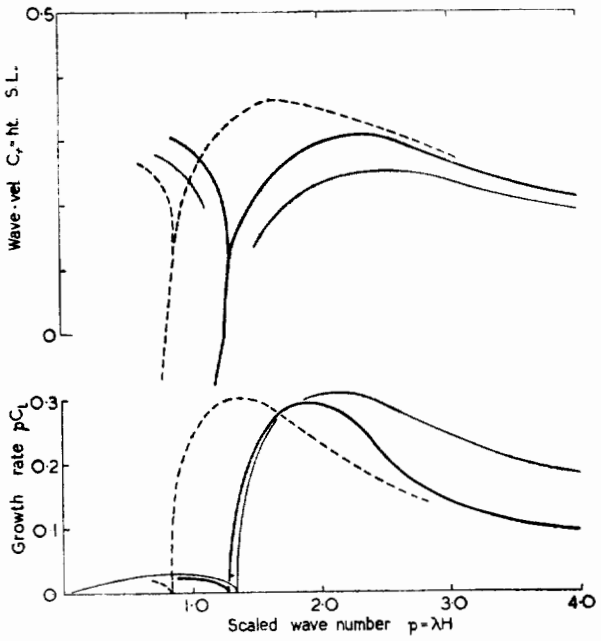

Figure 4. Growth-rate pc_i and wave speed as a function of wave-number for the linear velocity profile with $\gamma = 1$ and

Two rigid boundaries	$\kappa = 0$ (full lines).
Two rigid boundaries	$\kappa = 1$ (thin line).
Stratosphere with ratio of static stabilities 4 : 1	$\kappa = 0$ (dashed line)

$\gamma = 1$, the steering level is kept below the mid-level, and the spectrum is similar to the corresponding rigid lid spectrum, though with a bias towards longer waves (see Fig. 4 and Table 1). It is interesting to note that for $\gamma = 1$, the presence of this stratosphere leads to a slight increase in the maximum growth-rate, which is associated with the more symmetrical position of the steering level.

Unfortunately no calculations were made with $\gamma < 0$ which would correspond to easterly shear. We would expect that the waves would have their steering level and maximum amplitude displaced further towards the tropopause, with small amplitude at the ground.

6. Linear profile – mass divergence

The effect of the variation of density with height on the continuity equation is expressed in terms of the mass divergence parameter, κ. This mass divergence effect is implicitly included when pressure is used as the vertical coordinate, although there is then a corresponding complication in the form of the thermal wind-equation. Expanding the right-hand side of Eq. (1) we have :

$$\frac{D\zeta}{Dt_h} + v\beta = \frac{f}{\rho}\frac{\partial}{\partial Z}(\rho w) \simeq f\frac{\partial w}{\partial Z} + \frac{f}{\rho_0}\frac{d\rho_0}{dZ}w$$

It is easily seen that if v and w are positively correlated then the second term on the right enhances the β-effect. It has already been noted that the short waves are made unstable by the β-effect and we find this effect intensified for $\gamma\kappa > 0$ (see Fig. 4).

The steering level of the long waves is practically unchanged with respect to the pressure coordinate, so that with $\kappa > 0$, the steering level is lower. However, for these long waves it is found that the mass divergence does not contribute to the effect of the

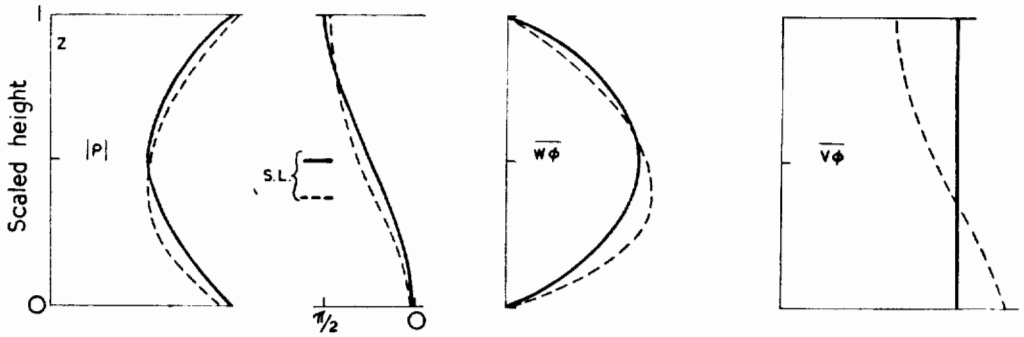

Figure 5. Perturbation pressure : amplitude and phase. Average over a wavelength of the upward and northward entropy transport for the dominant waves between two rigid boundaries when the unperturbed velocity profile is linear. With $\gamma = 0$ (full line) and $\gamma = 0{\cdot}5$ (dashed line). The amplitudes are expressed in arbitrary units and the steering levels, from Fig. 2, are denoted by S.L.

generalized β parameter given by the term $(\gamma + \kappa u')$ of Eq. (6). For example, with $\gamma = 0$ and any κ there is *no* critical wavelength, though if $\kappa \neq 0$ the short waves are unstable (contrast Fig. 2 where $\gamma\,\kappa = 0$ and the short waves are stable).

The amplitude of all waves is distorted (relative to $\kappa = 0$) so that the specific kinetic energy $\frac{1}{2}\rho\,\mathbf{V}^2$ is insensitive to the mass divergence effect.

7. Linear profile – the structure of the dominant wave

(a) *Shallow fluid*

With $\gamma \ll 1$ corresponding to a large shear, the proximity and nature of the boundaries is important. For example, with two rigid boundaries and dominant wave number p_x, then

$$p_x \simeq 1{\cdot}60 + 0{\cdot}6\,\gamma^2 \qquad (\gamma \ll 1)$$

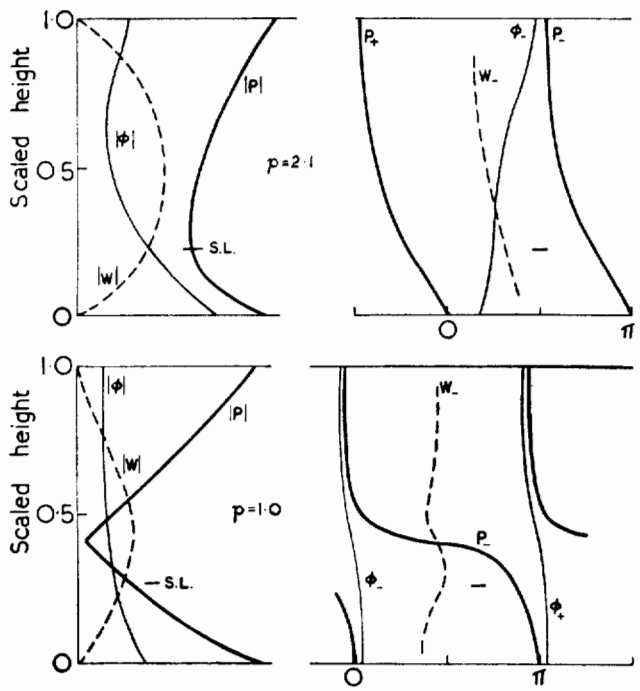

Figure 6. Amplitude and phase of perturbation pressure P, potential temperature ϕ, and vertical velocity w. Motion between two rigid boundaries with $\gamma = 1$, and linear velocity profile. Dominant wave $p = 2{\cdot}1$, 'Super-critical' wave $p = 1{\cdot}0$ (see Fig. 4).

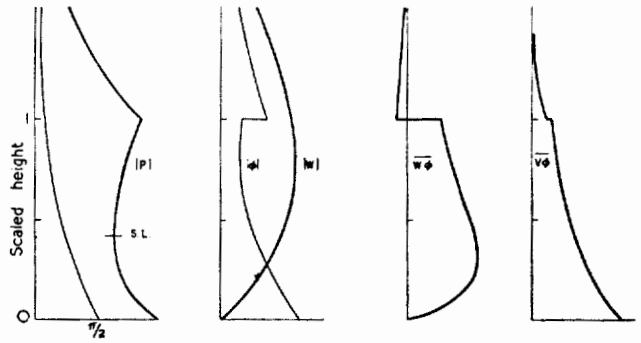

Figure 7. Phase and amplitude of pressure perturbation, amplitude of potential temperature and vertical velocity perturbations. Average upward and northward entropy transport (amplitudes on arbitrary scale). Dominant wave with stratosphere $B_S/B_T = 4$, $\gamma = 1$, and linear velocity profile.

With $\gamma < 1$, the pressure perturbation is nearly symmetrical about the mid-level of the fluid. The bias due to the β-effect occurs in the temperature field (through the stretching terms), and in the velocity field and shows more clearly in the entropy transport (see Fig. 5).

With $\gamma > 0$, and for near-dominant wavelengths, the wave amplitude decreases exponentially throughout the stratosphere, though rather longer waves may have maximum pressure perturbation just above the tropopause. Note (in Figs. 7 and 8) the temperature discontinuity at the tropopause level ($z = 1$). This indicates displacements of the tropopause that are in phase with the vertical displacement of a particle travelling (west-east, left to right) through the wave. Consequently the displaced tropopause is lowest near the upper trough. In the stratosphere the vertical velocity decreases less rapidly than the meridional velocity because of the large zonal particle velocity implied by the assumption of a constant thermal wind. Thus at great heights the particle paths will be almost vertical and the speeds small. In fact the calculations indicate a small downward flux of entropy in the stratosphere (Fig. 7).

(*b*) *Deep fluid*

For $\gamma \gg 1$, corresponding to small shear, the scale length is that associated with the β-effect, for the isentropic surfaces and therefore particle paths must be very nearly

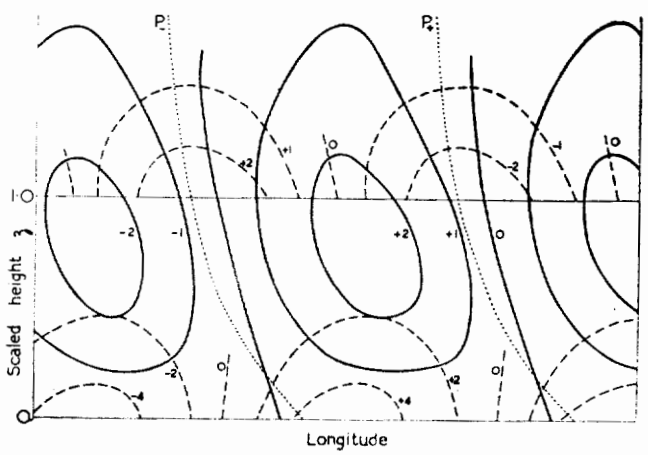

Figure 8. Zonal cross-section of the dominant wave, $\gamma = 1$ with 4 : 1 stratosphere as Fig. 7. Isopleths of potential temperature (dashed lines), and vertical velocity (thin lines), are expressed in arbitrary units.

horizontal. Thus the changes in the vorticity of a parcel of fluid are mainly those associated with meridional displacement and the variation of the Coriolis parameter, and only very close to a boundary does the stretching become significant. Thus for the dominant wave-number p_x,

$$p_x \simeq 0{\cdot}83\,\gamma\,(\gamma \gg 1).$$

The dominant wave is concentrated in the region up to the (low) steering level (Fig. 9) and variations at the upper boundary are unimportant.

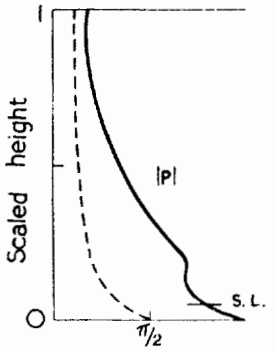

Figure 9. Pressure perturbation for the dominant wave, $\gamma = 5$, linear velocity profile. Phase (dashed) and amplitude (full line).

The maximum pc_i (conversion efficiency) varies very little: for $0 < \kappa < 1$, $0 < \gamma < 10$, and the presence of the 4 : 1 stratosphere, the variation is about 5 per cent.

The trough lines slope backwards (westwards) with height, and the total phase-lag varies from zero for very short waves to π (half-wavelength) for very long waves. However, the dominant waves are characterized by a phase-lag of nearly $\pi/4$ for large variations in the constraints. Table 1 gives a short list of dominant wave numbers as calculated for the linear velocity profile. p_1 is appropriate when the motion is bounded by two rigid boundaries, p_2 when the upper boundary is replaced by a semi-infinite layer with a static stability four times that of the lower fluid.

TABLE 1. WAVELENGTH OF THE MOST RAPIDLY AMPLIFYING WAVE, FOR DIFFERENT MODEL ATMOSPHERES

Dominant wave-number		p_1 with two lids	p_2 with 'stratosphere' 4 : 1
γ	κ	p_1	p_2
0	0	1·61	1·15
1	0	1·93	1·35
0	1	1·70	
1	1	2·18	

8. CURVED VELOCITY PROFILES

We now consider some modifications caused by the variations of thermal wind with height. For simplicity the mass divergence effect is neglected ($\kappa = 0$), and the motion is supposedly bounded by two rigid lids. Strictly the static stability is a function of height and latitude, but a constant value is assumed. This is consistent with the Richardson number being large, and is additionally appropriate because we shall be concerned with rather short waves in this section.

We may readily distinguish between two effects of shear variation.

(a) *Isolated wave*

The velocity profile may be such that a wave can exist without reference to material boundaries. The criterion for such isolated waves is similar to that given by Rayleigh for barotropic instability, i.e., growing waves may exist if $(\gamma - u'')$ changes sign, and the wave must have its steering level and maximum amplitude near the level of the zero. Note that only if $\gamma = 0$ does this correspond to a stationary value of the shear, or of available potential energy.

This class of wave is unlikely to be of direct importance for the one-dimensional profiles considered here, because the fluid is so shallow that the influence of at least one of the boundaries predominates.

(b) *Boundary waves*

A change in the sign of the shear may make it possible to have independent boundary waves such as the lower boundary wave discussed in connexion with the linear profile. Analysis of the short waves is instructive because they are able to 'pick out' ranges of height favourable for growth, and an analytic solution valid for very short waves has been derived. Criteria applicable to a two-lid model are given below:

$$\left.\begin{aligned} &\text{if } u'(\gamma + \kappa u' - u'') > 0 \text{ at } z = 0 \text{ (bottom)}, && \left(c \sim u_0 + \frac{1}{p} u_0' + i c_i\right) \\ &\text{if } u'(\gamma + \kappa u' - u'') < 0 \text{ at } z = 1 \text{ (top)}, && \left(c \sim u_1 - \frac{1}{p} u_1' + i c_i\right) \end{aligned}\right\} \quad . \quad (11)$$

then corresponding unstable solutions exist, with $c_i \simeq \frac{\pi}{e^2 p^2} |u'' - \kappa u' - \gamma|$ at the appropriate boundary. These formulae are valid as $p \to \infty$ and the mass divergence effect has been included temporarily.

Some calculations were made using a parabolic velocity profile, so that the isolated wave would not be present. The profile $u = 1{\cdot}5\, z^2 - z$ was chosen as representing roughly the easterly maximum in the Trade winds (Fig. 10). Note that $\int_0^1 (u')^2\, dz = 1$ so that the efficiency factor pc_i is comparable with that for the linear profile. Note however that the efficiency defined in the introduction properly refers to the *local* (maximum) entropy gradient.

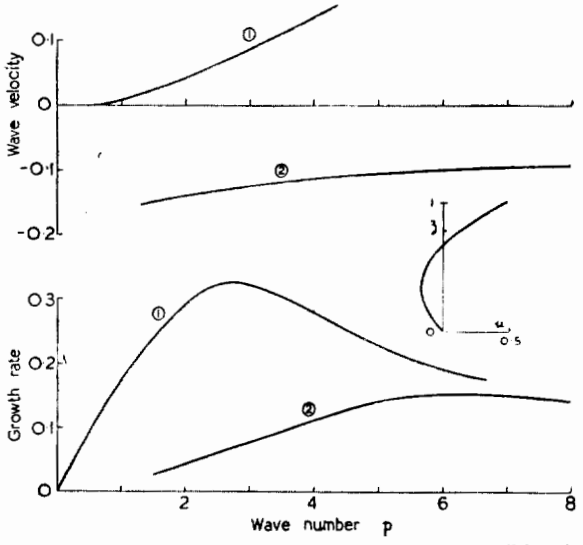

Figure 10. Growth-rate and wave velocity of each of the two waves possible with $u = 1{\cdot}5\, z^2 - z$, $\gamma = 0$, $\kappa = 0$; (1) upper wave; (2) lower wave.

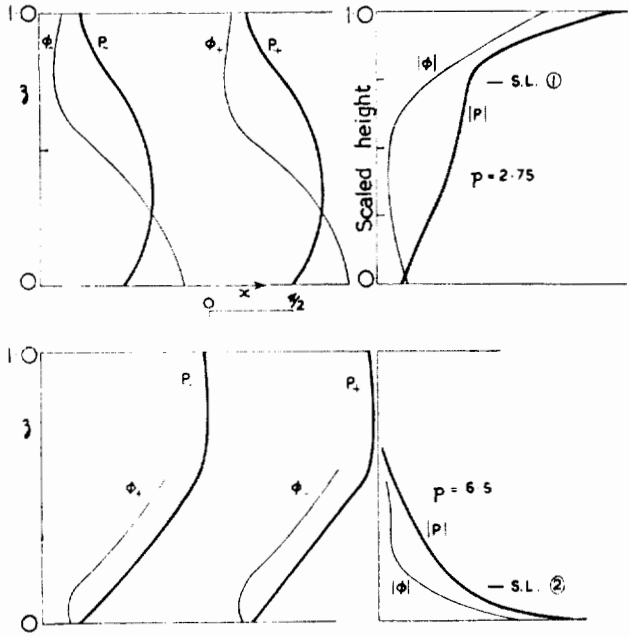

Figure 11. Phase and amplitude of pressure and potential temperature perturbations $u = 1{\cdot}5\,z^2 - z$, $\gamma = \kappa = 0$; (1) upper wave; (2) lower wave.

Each wave of Fig. 11 is similar to the uniform shear wave, but with the amplitude decreasing in the region where the Richardson number is large. The northward transport of entropy is in the opposite sense to the trough-line slope, so that the trough-line has, in general, the same shape as the mirror image of the velocity profile. Thus the lower wave (2) transports heat southwards, especially in the lower layers. Upper wave (1) transports heat northwards, especially in the upper layers. Note the short (horizontal and vertical) wavelength of the lower wave.

9. Note on the calculations

Most of the calculations were made using a layer-type model with simple (3 point) finite-difference approximations to the differentials. The differential equation of the form

$$F'' + \left(\frac{\gamma - u''}{u - c} - p^2\right) F = 0 \qquad . \qquad . \qquad . \qquad (12)$$

is replaced by a set of finite-difference equations :

$$F(z + h) - \left\{2 + h^2 p^2 - \frac{h^2(\gamma - u'')}{u - c}\right\} F(z) + F(z - h) = 0 \qquad . \qquad (13)$$

$z = nh$, $0 \leqslant n \leqslant N$ where $Nh = 1$ and h is the grid size.

The two boundary conditions in finite-difference form enable us to eliminate $F(-h)$ and $F(1 + h)$ (i.e., for motion between two rigid boundaries), thus leaving a set of $(N + 1)$ simultaneous equations for $(N + 1)$ values of $F(nh)$. The condition for a non-zero solution is that the determinant of the coefficients of $F(nh)$ should vanish, and since each equation is of the same form as Eq. (13), the determinant is a polynomial of degree $N + 1$ in c. But the differential equation has usually (for sub-critical wavelengths) only one pair of eigen values whereas the difference equation has $N + 1$ roots. Now if the

truncation errors are to be reduced, h must be made small, therefore N large, and the equation that has to be solved will have $N - 1$ spurious roots. The interference of these spurious solutions was reduced by solving with successively graded nets. A coarse network was used to locate c, the mesh-length was halved and this value used as a first approximation to the more accurate c. This procedure was continued until a sufficiently accurate value had been obtained, the parameters of the wave (e.g., p) were then changed and the process repeated.

It is a general characteristic of unspecialized numerical methods that these work best when the functions are smoothest : in this case when the growth-rate is large. On the other hand, analytic methods are usually most powerful when the function behaves violently in a limited region, i.e., near a singularity. Thus for regions of very small growth-rate (at the critical points, and for very short waves), the analytic methods were used. A judicious combination of both had to be used in order to obtain the complete spectrum.

A major source of error is the inability of the finite-difference approximations to cope with the exponential-type functions involved. For short wavelengths it is obvious that the functions involved are nearly linear combinations of exp $\pm pz$, but the 3-point finite-difference operation always overestimates the magnitude of the curvature of such a function. Even at $ph = 1$ the overestimation is 9 per cent, at $ph = 2$ it is 38 per cent. (The errors in the wave velocity are of the same order). It was found that for a given mesh size, the technique gave stable pairs of solutions for sufficiently short waves. Decreasing the mesh size results in an extension of the correct (i.e., unstable) solution.

A second, rather more spectacular error is associated with the nature of the singularity of the differential Eq. (12) where c is a complex number, and effectively we integrate this equation along the real axis from $z = 0$ to $z = 1$. Part of this integration involves $\int \frac{dz}{z - c}$ and if the imaginary part of c is small, this integral consists of a sum of large real values which cancel, plus a sum of small imaginary values which add to give a contribution $\pm i\pi$.

If this integration is approximated by using point values then the real part does not, in general, cancel, and unless a grid-point happens to be close to $z = c$ the imaginary part will be hardly noticed. Thus, not only is the integral badly represented near the steering level, but its value fluctuates according to the position of $z_1 =$ Real part c relative to the nearest grid-point. A rough analysis suggests that if the imaginary part of $c < h/4$ then this effect will be important. The effect was most interesting near the critical wavelengths, where the growth-rate is small, and where a small change in the wave-number results in a large change in the wave velocity.

Acknowledgments

I am indebted to Dr. E. T. Eady who advised, critized (and diverted) my attempts to solve this problem. I would like to thank the Department of Scientific and Industrial Research Organisation for a maintenance grant and the Armament Research and Development Establishment for allowing me to use their Ferranti II^x computer.

References

Charney, J. G. 1947 *J. Met.*, **4**, p. 135.
Eady, E. T. 1949 *Tellus*, **1**, p. 33.
Kuo, H. L. 1952 *J. Met.*, **9**, p. 260.